Available online at www.sciencedirect.com

ScienceDirect

International Journal of Solids and Structures 43 (2006) 7939–7958

INTERNATIONAL JOURNAL OF SOLIDS and STRUCTURES

www.elsevier.com/locate/ijsolstr

Non-element method of solving 2D boundary problems defined on polygonal domains modeled by Navier equation

Eugeniusz Zieniuk *, Agnieszka Boltuc

Department of Mathematics and Physics, Institute of Computer Science, University of Bialystok, 15-887 Bialystok, ul. Sosnowa 64, Poland

Received 28 July 2005; received in revised form 4 April 2006
Available online 22 April 2006

Abstract

The paper presents a non-element method of solving boundary problems defined on polygonal domains modeled by corner points. To solve these problems a parametric integral equation system (PIES) is used. The system is characterized by a separation of the approximation of boundary geometry from the approximation of boundary functions. This feature makes it possible to effectively investigate the convergence of the obtained solutions with no need of performing the approximation of boundary geometry. The testing examples included confirm high accuracy of the solutions.

Keywords: Elasticity; Navier equation; Boundary integral equation; Boundary element method (BEM); Parametric integral equation system (PIES)

1. Introduction

Solutions of linear problems of mechanics are often reduced to resolving Navier equation with posed boundary conditions. A variety of numerical methods have been used to solve these problems. Analytical methods, however, can be used only for some specific cases of boundary problems in mechanics (Lebedev et al., 1979; Timoshenko and Goodier, 1970). Currently they are mainly applied to test and verify dynamically developing numerical methods. Among the most commonly used numerical methods, at present, are the boundary element method (BEM) and finite element method (FEM). The methods, which make use of the so-called finite elements (Zienkiewicz, 1977) or boundary elements (Brebbia et al., 1984; Banerjee and Butterfield, 1981), allow us to create models of domains (boundaries) to solve practical problems dealing with various boundary conditions. The practicality and universality of these methods, should not, however, stop us from looking for new, even more effective methods, particularly useful for new types of boundary problems that are difficult to solve by means of currently available numerical methods.

Traditional BEM and FEM enable us to produce effective models of a great variety of domains using the so-called finite or boundary elements, which is their main advantage. However, their drawback lies in the

* Corresponding author. Fax: +48 85 745 7662.
E-mail addresses: ezieniuk@ii.uwb.edu.pl (E. Zieniuk), aboltuc@ii.uwb.edu.pl (A. Boltuc).

0020-7683/$ - see front matter
doi:10.1016/j.ijsolstr.2006.04.008

necessity of replacing the continuous domains (or boundaries) with discrete ones, which in practice requires, particularly in complex boundary problems, an introduction of a large number of input data (nodes) and also resolving a considerable number of algebraic equation systems. Each day brings some original research work presenting new developments in the field and it would be impossible to mention all of them here (Camp and Gipson, 1991; Jonston, 1996, 1997; Sen, 1995; Liggett and Salmon, 1981; Durodola and Fenner, 1990; Gray and Soucie, 1993; Singh and Kalra, 1995). It should be noted, however, that the main idea behind all these papers is an attempt to improve existing BEM and FEM based on the traditional discretization of the domain or its boundary.

In the research (Zieniuk, 2001, 2002) carried out by the author, a new approach to boundary problems has been proposed: an approach that would no longer require traditional boundary discretization or at least, eliminate its use to minimum. To make it possible, it is necessary to analytically modify the traditional boundary integral equation (BIE), which, in general, consists in getting rid of the necessity of defining the shape of the boundary by means of boundary integral. The expression resulting from the modification of the traditional BIE for the Laplace's and Helmholtz equations is called the parametric integral equation system (PIES) as the boundary geometry in the PIES kernels has been analytically defined in a parametric way (Zieniuk, 2003).

The solution of the PIES in a direct way is independent of the shape of the boundary geometry as the boundary is defined analytically in the PIES mathematical formalism (Zieniuk, 2003). In other words, in PIES the approximation of boundary geometry is independent of the approximation of boundary functions. Potentially, it creates greater possibilities of choosing more effective ways of both geometry modeling and choosing more effective methods of the approximation of the boundary functions. Thus, to practically define, for example, a polygonal domain, only corner points are posed (Zieniuk, 2002). The number of these points is considerably smaller than the number of nodes in the case of the traditional FEM. For curvilinear boundary shapes we use Bézier curves (Zieniuk, 2003) to obtain their continuous definition.

The effectiveness of PIES in solving both Laplace's (Zieniuk, 2002) and Helmholtz (Zieniuk et al., 2004; Zieniuk and Bołtuć, 2004) equations with various boundary conditions will naturally encourage us to generalize PIES for Navier equations. The advantage of the numerical solution of PIES compared to traditional BIE is the fact that (1) we need smaller number of data to define the boundary in a continuous and unequivocal way; (2) the solutions on the boundary are obtained in a continuous way with high exactness; (3) we have to solve a much smaller system of algebraic equations even in comparison with the traditional BEM; (4) the mathematical formalism of PIES makes it possible to carry out an easy modification of the boundary geometry in a continuous way (Zieniuk and Bołtuć, 2005).

The purpose of this paper is to obtain a PIES and propose a testing method of its numerical solution for 2D boundary problems on polygon domains modeled by Navier equations. Another interesting aspect of the problem is to investigate the effectiveness of PIES with respect to the modeling of boundary geometry and exactness of the solutions obtained. The numerical examples included in the paper confirm that in the case of Navier equations the proposed method shows both high accuracy and effectiveness compared with exact solutions and other numerical methods.

2. Modification of Somigliana's identity

Classical boundary integral equations (BIE) for elasticity theory are obtained form Somigliana's identity (Brebbia et al., 1984) for displacements. The identity both in its general form and the form suitable for further analytical modification, can be presented as follows:

$$\bar{u}(x) = \int_{\Gamma} U^*(x,y)p(y)\,\mathrm{d}\Gamma(y) - \int_{\Gamma} P^*(x,y)u(y)\,\mathrm{d}\Gamma(y) + \int_{\Omega} U^*(x,y)b(y)\,\mathrm{d}\Omega(y), \tag{1}$$

where

$$\bar{u}(x) = \begin{cases} u(x) & x \in \Omega \\ 0.5u(x) & \text{for } x \in \Gamma \\ 0 & x \neq \bar{\Omega} \end{cases}, \quad p(y) \equiv \frac{\partial u(y)}{\partial n(y)} \quad \text{and} \quad P^*(x,y) \equiv \frac{\partial U^*(x,y)}{\partial n(y)}.$$

The classical BIE is a specific form of this identity and is obtained when $x \in \Gamma$. In BIE boundary Γ is generally defined by the boundary integral, hence the numerical solution of BIE requires the modeling of real boundary for each specific boundary problem. When applying the boundary element method (BEM) for solving BIE various boundary elements are used to model the boundary (Brebbia et al., 1984; Banerjee and Butterfield, 1981).

In further analysis to simplify the Somigliana's identity (1) the last element accounting for mass forces is neglected. The integrand function $U^*(x,y) = [U^*_{ij}(x,y)],\ i,j = 1,2$ is the fundamental solution for the Navier equation and is represented by the following formula (Brebbia et al., 1984; Banerjee and Butterfield, 1981):

$$U^*_{ij}(x,y) = \frac{-1}{8\pi(1-\nu)\mu}\{(3-4\nu)\ln(r)\delta_{ij} - r_{,i}r_{,j}\}, \quad r_{,i} = \frac{\partial r}{\partial y_i}, \tag{2}$$

where μ is the Lame constant, δ_{ij} is the Kronecker symbol, $r = [(y_1 - x_1)^2 + (y_2 - x_2)^2]^{0.5}$.

In the theory of elasticity function (2) is known as Kelvin's solution. The other integrand $P^*(x,y) = [P^*_{ij}(x,y)],\ i,j = 1,2$ in formula (1) expresses the components of the stress vector and is represented by the following formula:

$$P^*_{ij}(x,y) = \frac{-1}{4\pi(1-\nu)r}\left\{[(1-2\nu)\delta_{ij} + 2r_{,i}r_{,j}]\frac{\partial r}{\partial n} - (1-2\nu)(r_{,i}n_j - r_{,j}n_i\right\}. \tag{3}$$

Knowing the distribution of both the displacements $u(y) = [u_1(y), u_2(y)]^{\mathrm{T}}$ and surface forces $p(y) = [p_1(y), p_2(y)]^{\mathrm{T}}$ on the boundary, and using formula (1) it is possible to determine the displacement distribution at any given point of domain Ω.

The accuracy of the solutions in domain Ω depends, however, on two factors: (1) approximation accuracy of the displacement (or surface forces) on the boundary and (2) approximation accuracy of the shape of the boundary geometry. Hence it seems reasonable to modify the traditional BIE in such a way as to obtain an independent boundary approximation of the unknown functions in the numerical solution. In other words, it enables us to independently choose the most convenient methods of boundary geometry modeling, depending on its complexity without any intrusion into approximation of boundary functions and vice versa.

Due to above, we deal with the analytical modification of the traditional BIE first so that the boundary geometry is not defined by boundary integral but is included in the mathematical formalism of the expression which is obtained after the modification of BIE.

2.1. Fourier transformation of Somigliana's identity

The modification of the traditional BIE for the theory of elasticity is, however, more complex than the previously performed modification for the potential problems modeled by the Laplace's equation (Zieniuk, 2001, 2003). Considering the fact that the modification remains analogical, the way it is carried out is also similar. To do that, it is necessary to adapt Fourier transform to Somigliana's identity (1). Having done that, we obtain:

$$\hat{\hat{u}}(\xi) = \int_\Gamma \widehat{U}^*(\xi,y)p(y)\,\mathrm{d}\Gamma(y) - \int_\Gamma \widehat{P}^*(\xi,y)u(y)\,\mathrm{d}\Gamma(y), \tag{4}$$

where $\widehat{U}^*(\xi,y)$ is the transform of the fundamental solution, whereas $\widehat{P}^*(\xi,y)$ is the transform of the singular solution in the domain of Fourier transforms for the Navier equation. The solutions for 2D problems of the elasticity theory can be shown in the following form:

$$\widehat{U}^*(\xi,y) = L^{-1}(\xi)\mathrm{e}^{-\mathrm{i}(\xi_1 y_1 + \xi_2 y_2)}, \tag{5}$$

$$\widehat{P}^*(\xi,y) = -\mathrm{i}[\xi_1 n_1(y) + \xi_2 n_2(y)]L^{-1}(\xi)\mathrm{e}^{-\mathrm{i}(\xi_1 y_1 + \xi_2 y_2)}, \tag{6}$$

where

$$L^{-1}(\xi)=\begin{bmatrix}\dfrac{2(1-\nu)|\xi|^2-\xi_1^2}{2\mu(1-\nu)|\xi|^4} & \dfrac{-\xi_1\xi_2}{2\mu(1-\nu)|\xi|^4}\\ \dfrac{-\xi_1\xi_2}{2\mu(1-\nu)|\xi|^4} & \dfrac{2(1-\nu)|\xi|^2-\xi_2^2}{2\mu(1-\nu)|\xi|^4}\end{bmatrix},\quad |\xi|^2=|\xi_1^2+\xi_2^2|. \tag{7}$$

Accounting for both fundamental (5) and singular (6) solutions in (4) we obtain the following expression in the domain of Fourier transforms:

$$\hat{\tilde{u}}(\xi)=L^{-1}(\xi)\tilde{p}(\xi)+\mathrm{i}L^{-1}(\xi)\{\xi_1\tilde{u}\tilde{n}_1(\xi)+\xi_2\tilde{u}\tilde{n}_2(\xi)\}, \tag{8}$$

where boundary functions $\tilde{p}(\xi)$ and $\tilde{u}\tilde{n}_m(\xi),\ m=1,2$ are represented by boundary integral equation:

$$\tilde{p}(\xi)=\int_\Gamma \mathrm{e}^{-\mathrm{i}(\xi_1 y_1+\xi_2 y_2)}p(y)\,\mathrm{d}\Gamma(y), \tag{9}$$

$$\tilde{u}\tilde{n}_m(\xi)=\int_\Gamma \mathrm{e}^{-\mathrm{i}(\xi_1 y_1+\xi_2 y_2)}n_m(y)u(y)\,\mathrm{d}\Gamma(y),\quad m=1,2\ \ y\in\Gamma. \tag{10}$$

It can be observed that there is a separation of the boundary from the domain in Eq. (8). The boundary is defined by the formalism of boundary integrals (9) and (10).

We use integral (10) to define the function transform $\tilde{u}\tilde{n}_m(\xi)$ on the boundary Γ. The unknown integrand $u(y)$ in (10) may be defined by means of the following Fourier formula:

$$u(y)=\frac{1}{4\pi^2}\int_{R^2}\mathrm{e}^{\mathrm{i}(\omega_1 y_1+\omega_2 y_2)}\hat{u}(\omega)\,\mathrm{d}\omega,\quad \omega\equiv(\omega_1,\omega_2), \tag{11}$$

where the integrand $\hat{u}(\omega)$ is given by

$$\hat{u}(\omega)=2[L^{-1}(\omega)\tilde{p}(\omega)+\mathrm{i}L^{-1}(\omega)\{\omega_1\tilde{u}\tilde{n}_1(\omega)+\omega_2\tilde{u}\tilde{n}_2(\omega)\}]. \tag{12}$$

The formula (12) is a particular case of the transform (8).

2.2. Modeling of boundary geometry in the mathematical formalism of Somigliana's identity

After substituting (12) into (11) – and then the resulting expression into (10) – we get the convolution integral equation in the domain of Fourier transforms:

$$\tilde{u}\tilde{n}_m(\xi)=\int_{R^2}\tilde{K}_m(\gamma_1,\gamma_2)L^{-1}(\omega)\{\tilde{p}(\omega)+\mathrm{i}[\omega_1\tilde{u}\tilde{n}_1(\omega)+\omega_2\tilde{u}\tilde{n}_2(\omega)]\}\,\mathrm{d}\omega, \tag{13}$$

where the kernel is

$$\widetilde{K}_m(\gamma_1,\gamma_2)=\frac{1}{4\pi^2}\int_\Gamma \mathrm{e}^{\mathrm{i}(\gamma_1 y_1+\gamma_2 y_2)}n_m(y)\,\mathrm{d}\Gamma(y),\quad \gamma_i=\omega_i-\xi_i. \tag{14}$$

The contour integral in (14) takes into consideration the boundary geometry of Γ. In our further considerations we divide the boundary Γ into n linear segments.

Therefore, after taking into consideration the segmental representation of the boundary, we may present the kernel (14) as

$$\widetilde{K}_m(\gamma_1,\gamma_2)=\frac{1}{4\pi^2}\sum_{p=1}^{n}\int_{\Gamma_p}\mathrm{e}^{\mathrm{i}(\gamma_1 y_1+\gamma_2 y_2)}n_m^{(p)}(y)\,\mathrm{d}\Gamma(y), \tag{15}$$

whereas the boundary transforms $\tilde{u}\tilde{n}_m(\xi)$ on the left-hand side of (13) may be represented in the following form:

$$\tilde{u}\tilde{n}_m(\xi)=\sum_{p=1}^{n}\tilde{u}_p\tilde{n}_m^{(p)}(\xi). \tag{16}$$

We denote the boundary transforms $\tilde{p}(\omega)$ and $\tilde{u}\tilde{n}_m(\omega)$ on individual segments on the right-hand side of (13) by the index r in the following way:

$$\tilde{p}(\omega) = \sum_{r=1}^{n} \tilde{p}_r(\omega), \quad \tilde{u}\tilde{n}_m(\omega) = \sum_{r=1}^{n} \tilde{u}_r \tilde{n}_m^{(r)}(\omega). \tag{17}$$

After substituting (17), (16) and (15) in (13) we obtain the following system of the convolution integral equations:

$$\tilde{u}_p \tilde{n}_m^{(p)}(\xi) = \int_{R^2} \overline{\overline{K}}_m(\gamma_1, \gamma_2) \sum_{r=1}^{n} L^{-1}(\omega)\{\tilde{p}_r(\omega) + \mathrm{i}[\omega_1 \tilde{u}_r \tilde{n}_1^{(r)}(\omega) + \omega_2 \tilde{u}_r \tilde{n}_2^{(r)}(\omega)]\}\, \mathrm{d}\omega, \tag{18}$$

where

$$\overline{\overline{K}}_m(\gamma_1, \gamma_2) = \frac{1}{4\pi^2} \int_{\Gamma_p} \mathrm{e}^{\mathrm{i}(\gamma_1 y_1 + \gamma_2 y_2)} n_m^{(p)}(y)\, \mathrm{d}\Gamma(y), \quad p = 1, 2, \ldots, n. \tag{19}$$

These boundary transforms on individual segments in (18) may be defined as follows:

$$\tilde{p}_r(\omega) = \int_{\Gamma_r} \mathrm{e}^{-\mathrm{i}(\omega_1 y_1 + \omega_2 y_2)} p_r(y)\, \mathrm{d}\Gamma(y), \tag{20}$$

$$\tilde{u}_k \tilde{n}_m^{(k)}(\omega) = \int_{\Gamma_k} \mathrm{e}^{-\mathrm{i}(\omega_1 y_1 + \omega_2 y_2)} n_m^{(k)}(y) \tilde{u}_k(y)\, \mathrm{d}\Gamma(y), \quad \omega = \xi, \ \ k = p, r. \tag{21}$$

In integrals (19)–(21) boundary geometry is still defined in a general way with the help of segment contour integrals. However, this way of boundary definition is very convenient to define it by appropriate functions.

2.3. Practical definition of polygon domains by corner points

In our further considerations concerning BIE modification, we shall concentrate exclusively on boundaries whose domains are polygonal in shape. To define such domains in the most exact and effective way, it is merely necessary to pose n corner points, as shown in Fig. 1.

This is the lowest number of input data required for unambiguous definition of the analyzed domain. An important characteristics of this method of domain definition is that the number of those points is independent of the length of the linear segments between these points. In other words, the number of the points for the geometrically identical domain is independent of its surface area. Another advantage of the method is the ease of domain modification, which is carried out simply by moving corner points. These are very important advantages over the traditional FEM and BEM, in which the number of elements is clearly dependent on the surface area of the analyzed domain and each modification of the domain requires a new discretization.

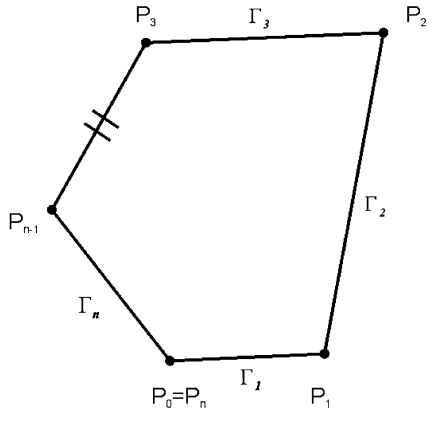

Fig. 1. Modeling of polygon domains by corner points.

Next, we assume that the linear segments Γ_r between the corner points are mathematically defined by parametric linear functions $\Gamma_r^{(1)}(s), \Gamma_r^{(2)}(s)$ with parameter s. Hence these functions must be taken into account in boundary transforms (19)–(21), in which the boundary is defined in a general way by means of segmental contour integrals Γ_r.

The kernel (19) for the boundary segments in the linear representation is described by the following formula:

$$\overline{\widetilde{K}}_m(\gamma_1,\gamma_2) = \frac{1}{4\pi^2} J_p \int_{s_{p-1}}^{s_p} \mathrm{e}^{\mathrm{i}[\gamma_1 \Gamma_p^{(1)}(s)+\gamma_2 \Gamma_p^{(2)}(s)]} n_m \,\mathrm{d}s, \quad s_{p-1} \leqslant s \leqslant s_p, \tag{22}$$

where

$$J_p = \left[\left(\frac{\partial y_1}{\partial s} \right)^2 + \left(\frac{\partial y_2}{\partial s} \right)^2 \right]^{0.5}, \quad y_1 = \Gamma_p^{(1)}(s), \;\; y_2 = \Gamma_p^{(2)}(s).$$

The segmental transforms $\tilde{p}_r(\omega)$, $\tilde{u}_k \tilde{n}_m^{(k)}(\omega)$ after considering linear segments have the following form:

$$\begin{aligned} \tilde{p}_r(\omega) &= J_r \int_{s_{r-1}}^{s_r} \mathrm{e}^{-\mathrm{i}[\omega_1 \Gamma_r^{(1)}(s)+\omega_2 \Gamma_r^{(2)}(s)]} p_r(s)\,\mathrm{d}s, \\ \tilde{u}_k \tilde{n}_m^{(k)}(\omega) &= J_k \int_{s_{k-1}}^{s_k} \mathrm{e}^{-\mathrm{i}[\omega_1 \Gamma_p^{(1)}(s)+\omega_2 \Gamma_p^{(2)}(s)]} \tilde{u}_k(s) n_m^{(k)}\,\mathrm{d}s, \quad \omega = \xi, \;\; k = p, r, \end{aligned} \tag{23}$$

where

$$p_r(s) = p_r[\Gamma_r^{(1)}(s), \Gamma_r^{(2)}(s)], \quad n_m^{(p)} = n_m^{(p)}[\Gamma_p^{(1)}(s), \Gamma_p^{(2)}(s)], \quad \tilde{u}_p(s) = \tilde{u}_p[\Gamma_p^{(1)}(s), \Gamma_p^{(2)}(s)].$$

To define the polygon domain we practically need to pose the coordinates of corner points P_i, $i = 0, 1, 2, \ldots, n$ of the polygon. The points are automatically used to create parametrical linear functions $\Gamma_p(s)$, which are used to mathematically define the segments between the corner points in the integrals (22) and (23).

3. One-dimensional parametrical system of integral equation

Having considered (23) and (22) in (18) and after applying inverse Fourier transformation, the integral equation system (18) after some complex transformations takes the form of

$$0.5 u_p(s_1) = \sum_{r=1}^{n} J_r \int_{s_{r-1}}^{s_r} \{ \overline{U}_{pr}^*(s_1,s) p_r(s) - \overline{P}_{pr}^*(s_1,s) u_r(s) \}\,\mathrm{d}s, \quad s_{p-1} \leqslant s_1 \leqslant s_p, \;\; s_{r-1} \leqslant s \leqslant s_r. \tag{24}$$

The expression (24) obtained here, as in earlier papers, has been called the parametric integral equation system (PIES) for Somigliana's identity. The kernels in this system are functions $\overline{U}_{pr}^*(s_1,s)$ and $\overline{P}_{pr}^*(s_1,s)$. The first integrand $\overline{U}_{pr}^*(s_1,s)$ is represented by the following integral expression:

$$\overline{U}_{pr}^*(s_1,s) = \frac{1}{4\pi^2} \int_{R^2} \mathrm{e}^{\mathrm{i}(\omega_1 \eta_1 + \omega_2 \eta_2)} L^{-1}(\omega)\,\mathrm{d}\omega, \tag{25}$$

where $\eta_1 = \Gamma_r^{(1)}(s) - \Gamma_p^{(1)}(s_1)$ and $\eta_2 = \Gamma_r^{(2)}(s) - \Gamma_p^{(2)}(s_1)$.

Having calculated integral (25) we obtain an expression in an explicit form, which due to the inclusion of the shape of boundary geometry in its formalism, is called a modified fundamental boundary solution for Navier equation.

The other integrand $\overline{P}_{pr}^*(s_1,s)$ in (24) is represented by the following expression:

$$\overline{P}_{pr}^*(s_1,s) = \overline{P}_1(s_1,s) n_1 + \overline{P}_2(s_1,s) n_2, \tag{26}$$

in which individual elements are calculated on the basis of integral expression:

$$\overline{P}_k(s_1,s) = \frac{-\mathrm{i}}{4\pi^2} \int_{R^2} \mathrm{e}^{\mathrm{i}(\omega_1 \eta_1 + \omega_2 \eta_2)} \omega_k L^{-1}(\omega)\,\mathrm{d}\omega, \quad k = 1, 2, \tag{27}$$

where $\eta_1 = \Gamma_r^{(1)}(s) - \Gamma_p^{(1)}(s_1)$ and $\eta_2 = \Gamma_r^{(2)}(s) - \Gamma_p^{(2)}(s_1)$.

Having calculated integral (27) and after its substitution into (26) we obtain an explicit expression that is called a modified singular boundary solution.

3.1. Modified fundamental and singular solutions for Navier equation

Boundary problems in the theory of elasticity can be resolved using integral boundary system (24). A practical application of the system is possible after obtaining the kernels from formulas (25) and (26) in explicit forms. To obtain the first kernel i.e. fundamental boundary solution, it is necessary to calculate integral (25):

$$\overline{U}^*_{pr}(s_1,s)=\frac{1}{4\pi^2}\int_{R^2}\mathrm{e}^{\mathrm{i}(\omega_1\eta_1+\omega_2\eta_2)}L^{-1}(\omega)\,\mathrm{d}\omega, \tag{28}$$

where $\eta_1=\Gamma^{(1)}_r(s)-\Gamma^{(1)}_p(s_1)$ and $\eta_2=\Gamma^{(2)}_r(s)-\Gamma^{(2)}_p(s_1)$.

The integrand $L^{-1}(\omega)$ is represented by matrix (7) in which variable ξ is changed into ω. As a result we obtain:

$$L^{-1}(\omega)=\begin{bmatrix}\dfrac{2(1-\nu)|\omega|^2-\omega_1^2}{2\mu(1-\nu)|\omega|^4} & \dfrac{-\omega_1\omega_2}{2\mu(1-\nu)|\omega|^4}\\ \dfrac{-\omega_1\omega_2}{2\mu(1-\nu)|\omega|^4} & \dfrac{2(1-\nu)|\omega|^2-\omega_2^2}{2\mu(1-\nu)|\omega|^4}\end{bmatrix},\quad |\omega|^2=|\omega_1^2+\omega_2^2|. \tag{29}$$

The other kernel i.e. singular boundary solution is obtained from formula (26):

$$\overline{P}^*_{pr}(s_1,s)=\overline{P}_1(s_1,s)n_1+\overline{P}_2(s_1,s)n_2, \tag{30}$$

in which individual elements are obtained after calculating integral:

$$\overline{P}_k(s_1,s)=\frac{-\mathrm{i}}{4\pi^2}\int_{R^2}\mathrm{e}^{\mathrm{i}(\omega_1\eta_1+\omega_2\eta_2)}\omega_k L^{-1}(\omega)\,\mathrm{d}\omega,\quad k=1,2. \tag{31}$$

To calculate the integrals we use both the residual method and the tables to inverse the Fourier transformation of functions. Having carried out some complex calculations (28) (see Appendix I) we obtain a modified fundamental solution in an explicit form for Navier equation:

$$\overline{U}^*_{pr}(s_1,s)=-\frac{1}{8\pi(1-\nu)\mu}\begin{bmatrix}(3-4\nu)\ln(\eta)-\dfrac{\eta_1^2}{\eta^2} & -\dfrac{\eta_1\eta_2}{\eta^2}\\ -\dfrac{\eta_1\eta_2}{\eta^2} & (3-4\nu)\ln(\eta)-\dfrac{\eta_2^2}{\eta^2}\end{bmatrix}, \tag{32}$$

where $\eta=[\eta_1^2+\eta_2^2]^{0.5}$, $\eta_1=\Gamma^{(1)}_r(s)-\Gamma^{(1)}_p(s_1)$ and $\eta_2=\Gamma^{(2)}_r(s)-\Gamma^{(2)}_p(s_1)$.

After calculating integral (31) (see Appendix II) and taking into account in (30) we obtain an explicit form of singular boundary solution, which can be presented as follows:

$$\overline{P}^*_{pr}(s_1,s)=-\frac{1}{4\pi(1-\nu)r}\begin{bmatrix}P_{11} & P_{12}\\ P_{21} & P_{22}\end{bmatrix},\quad p,r=1,2,\ldots,n, \tag{33}$$

where

$$P_{11}=\left\{(1-2\nu)+2\frac{\eta_1^2}{\eta^2}\right\}\frac{\partial\eta}{\partial n},\quad P_{12}=\left\{2\frac{\eta_1\eta_2}{\eta^2}\frac{\partial\eta}{\partial n}-(1-2\nu)\left[\frac{\eta_1}{\eta}n_2+\frac{\eta_2}{\eta}n_1\right]\right\},$$

$$P_{21}=\left\{2\frac{\eta_2\eta_1}{\eta^2}\frac{\partial\eta}{\partial n}-(1-2\nu)\left[\frac{\eta_2}{\eta}n_1+\frac{\eta_1}{\eta}n_2\right]\right\},\quad P_{22}=\left\{(1-2\nu)+2\frac{\eta_2^2}{\eta^2}\right\}\frac{\partial\eta}{\partial n},$$

$$\frac{\partial\eta}{\partial n}=\frac{\partial\eta_1}{\partial\eta}n_1+\frac{\partial\eta_2}{\partial\eta}n_2.$$

The obtained expressions (32) and (33) are kernels for PIES (24), which, unlike classical kernels, account for boundary geometry defined by parametrical linear functions in their mathematical formalism. Hence the PIES is not defined on the boundary as the traditional BIE but on the straight line in the parametric reference system. The resolution of the PIES is reduced simply to the approximation of boundary functions, hence we assume that the resolution no longer depends on the approximation of boundary geometry.

4. Resolution in domain

Having obtained the solution on the boundary by PIES, we can obtain solutions in domain Ω after an appropriate adaptation of Somigliana's identity. To do that, we use the transform represented by formula (8):

$$\hat{\tilde{u}}(\xi) = L^{-1}(\xi)\tilde{p}(\xi) + \mathrm{i}L^{-1}(\xi)\{\xi_1\tilde{u}\tilde{n}_1(\xi) + \xi_2\tilde{u}\tilde{n}_2(\xi)\}. \tag{34}$$

In this transform, boundary integrals $\tilde{p}(\xi)$, $\tilde{u}\tilde{n}_m(\xi)$, $m = 1, 2$ are represented by formulas (17) in which segment integrals can be presented by expressions (23) where variable ω is replaced by ξ. Thus finally we obtain:

$$\begin{aligned}
\tilde{p}_r(\xi) &= J_r \int_{s_{r-1}}^{s_r} \mathrm{e}^{-\mathrm{i}[\xi_1 \Gamma_l^1(s) + \xi_2 \Gamma_l^2(s)]} p_r(s)\,\mathrm{d}s, \\
\tilde{u}_r\tilde{n}_m^{(r)}(\xi) &= J_r \int_{s_{r-1}}^{s_r} \mathrm{e}^{-\mathrm{i}[\xi_1 \Gamma_l^1(s) + \xi_2 \Gamma_l^2(s)]} n_m^{(r)} \tilde{u}(s)\,\mathrm{d}s.
\end{aligned} \tag{35}$$

Having considered (35) in (17) and then the obtained expression in (34) and using the inverse Fourier transform we obtain the following expression:

$$u(x) = \sum_{r=1}^{n} J_r \int_{s_{r-1}}^{s_r} \left\{ \widehat{\overline{U}}_r^*(x,s) p_r(s) - \widehat{\overline{P}}_r^*(x,s) u_r(s) \right\} \mathrm{d}s, \quad s_{r-1} \leqslant s \leqslant s_r. \tag{36}$$

The first integrand $\widehat{\overline{U}}_r^*$ is calculated form the integral expression:

$$\widehat{\overline{U}}_r^*(x,s) = \frac{1}{4\pi^2} \int_{R^2} \mathrm{e}^{\mathrm{i}(\xi_1 \overleftrightarrow{r}_1 + \xi_2 \overleftrightarrow{r}_2)} L^{-1}(\xi)\,\mathrm{d}\xi, \tag{37}$$

where $\overleftrightarrow{r}_1 = \Gamma_r^{(1)}(s) - x_1$ and $\overleftrightarrow{r}_2 = \Gamma_r^{(2)}(s) - x_2$.

Substituting matrix (29) into formula (37) and performing a relatively complex integration, we obtain an integrand in the following matrix form:

$$\widehat{\overline{U}}_r^*(x,s) = -\frac{1}{8\pi(1-\nu)\mu} \begin{bmatrix} (3-4\nu)\ln(\overleftrightarrow{r}) - \dfrac{\overleftrightarrow{r}_1^2}{\overleftrightarrow{r}^2} & -\dfrac{\overleftrightarrow{r}_1 \overleftrightarrow{r}_2}{\overleftrightarrow{r}^2} \\ -\dfrac{\overleftrightarrow{r}_1 \overleftrightarrow{r}_2}{\overleftrightarrow{r}^2} & (3-4\nu)\ln(\eta) - \dfrac{\overleftrightarrow{r}_2^2}{\overleftrightarrow{r}^2} \end{bmatrix}, \tag{38}$$

where $\overleftrightarrow{r} = [\overleftrightarrow{r}_1^2 + \overleftrightarrow{r}_2^2]^{0.5}$, $\overleftrightarrow{r}_1 = \Gamma_r^{(1)}(s) - x_1$ and $\overleftrightarrow{r}_2 = \Gamma_r^{(2)}(s) - x_2$.

The other integrand $\widehat{\overline{P}}_r^*$ in (36) is represented by the following expression:

$$\widehat{\overline{P}}_r^*(x,s) = \widehat{\overline{P}}_1(x,s) n_1 + \widehat{\overline{P}}_2(x,s) n_2, \tag{39}$$

in which individual elements are calculated by the following integral:

$$\widehat{\overline{P}}_k(x,s) = \frac{-\mathrm{i}}{4\pi^2} \int_{R^2} \mathrm{e}^{\mathrm{i}(\xi_1 \overleftrightarrow{r}_1 + \xi_2 \overleftrightarrow{r}_2)} \xi_k L^{-1}(\xi)\,\mathrm{d}\xi, \quad k = 1, 2. \tag{40}$$

After the integration we obtain an explicit form of integrand $\widehat{\overline{P}}_r^*$, whose matrix form is as follows:

$$\widehat{\overline{P}}_r^*(x,s) = -\frac{1}{4\pi(1-\nu)\overleftrightarrow{r}} \begin{bmatrix} P_{11} & P_{12} \\ P_{21} & P_{22} \end{bmatrix}, \quad r = 1, 2, 3, \ldots, n, \tag{41}$$

where

$$P_{11} = \left\{ (1-2\nu) + 2\frac{\overleftrightarrow{r}_1^2}{\overleftrightarrow{r}^2} \right\} \frac{\partial \overleftrightarrow{r}}{\partial n}, \quad P_{12} = \left\{ 2\frac{\overleftrightarrow{r}_1 \overleftrightarrow{r}_2}{\overleftrightarrow{r}^2} \frac{\partial \overleftrightarrow{r}}{\partial n} - (1-2\nu) \left[\frac{\overleftrightarrow{r}_1}{\eta} n_2 + \frac{\overleftrightarrow{r}_2}{\eta} n_1 \right] \right\},$$

$$P_{21} = \left\{ 2\frac{\overleftrightarrow{r}_2 \overleftrightarrow{r}_1}{\overleftrightarrow{r}^2} \frac{\partial \overleftrightarrow{r}}{\partial n} - (1-2\nu) \left[\frac{\overleftrightarrow{r}_2}{\eta} n_1 + \frac{\overleftrightarrow{r}_1}{\eta} n_2 \right] \right\}, \quad P_{22} = \left\{ (1-2\nu) + 2\frac{\overleftrightarrow{r}_2^2}{\overleftrightarrow{r}^2} \right\} \frac{\partial \overleftrightarrow{r}}{\partial n},$$

$$\frac{\partial \overleftrightarrow{r}}{\partial n} = \frac{\partial \overleftrightarrow{r}_1}{\partial \overleftrightarrow{r}} n_1 + \frac{\partial \overleftrightarrow{r}_2}{\partial \overleftrightarrow{r}} n_2.$$

The integrands (38) and (41), as in earlier papers (Zieniuk, 2002), have been called fundamental and singular solutions in domain for Navier equation respectively.

5. Numerical solution of PIES for Navier equation

The PIES obtained in Section 3.1 is characterized by the fact that it contains analytically defined boundary geometry. Practical definition of the shape of the polygonal boundary geometry is simply reduced to posing the coordinates for corner points. As a result we can assume that the boundary geometry has been simply included in PIES. The next step is the approximation of boundary functions, which, in this case, means solving the PIES obtained. That is why the resolution of PIES is no longer directly related to boundary geometry, as PIES is defined on the straight line in the parametrical system of reference.

The separation of the approximation of boundary geometry form the approximation of boundary functions creates greater possibilities of more effective approximation of boundary functions. Generally the separation gives a possibility of applying traditional numerical methods (Fletcher, 1984) used for solving differential and integral equations. It also enables us to search for even more effective methods suited to different types of boundary problems.

In earlier papers (Zieniuk et al., 2004; Zieniuk and Bołtuć, 2004) to solve the PIES obtained for Laplace and Helmholtz equations, a collocation method (Fletcher, 1984) was used. As the method turned out to be very effective and simple in a number tested cases, it was decided to apply it for solving the PIES obtained for Navier equation. The method consists in approximating boundary functions $u_r(s)$, $p_r(s)$ on each segment r, by means of the following:

$$p_r(s) = \sum_{k=0}^{N} p_r^{(k)} T_r^{(k)}(s), \quad u_r(s) = \sum_{k=0}^{N} u_r^{(k)} T_r^{(k)}(s), \tag{42}$$

where $u_r^{(k)}, p_r^{(k)}$ are unknown coefficients, N is a number of coefficients on segment r, and $T_r^k(s)$ are the global base functions on individual segments – Chebyshev polynomials.

The unknown coefficients for one of the approximation series (42) on each segment are obtained as a result of an interpolation of posed boundary conditions. Coefficients of the second series are obtained after solving the PIES. After the substitution of (42) into (24) we obtain an expression for any given boundary conditions in the following general form:

$$0.5u_p(s_1) = \sum_{r=1}^{n} \sum_{k=0}^{N} \left\{ p_r^{(k)} \int_{s_{r-1}}^{s_j} \overline{U}_{pr}^*(s_1, s) - u_r^{(k)} \int_{s_{r-1}}^{s_r} \overline{P}_{pr}^*(s_1, s) \right\} T_r^{(k)}(s) J_r \, \mathrm{d}s. \tag{43}$$

After fulfilling the equation at collocation points $s_1 = s_{1_{(r)}}$ $(r = 1, 2, 3, \ldots, M)$, $M = n \times N$, (total number of collocation points M is a product of number of segments n and number of unknown coefficients N on individual segments), we obtain an algebraic equation system with respect to unknown coefficients $p_j^{(k)}$ or $u_j^{(k)}$. On solving that equation we obtain unknown coefficients from one of the approximation series (42). After substituting the coefficients into (42), an analytical expression for the unknown boundary function is obtained. From that expression we can obtain solutions at any given point for any boundary segment.

The accuracy of the results obtained by that method is largely dependent on N and also the way of arranging collocation points and the complexity of posed boundary conditions. Congruent with earlier researches for Laplace's equation, the most accurate results were obtained when extreme collocation points were placed close

to the ends of segments (Zieniuk et al., 2004). Solutions of high accuracy were obtained even for a much smaller algebraic equation system than in the case of traditional BEM (Zieniuk, 2001).

The proposed method is very simple from the programmatic point of view and effective in practical applications. It enables both optimal arrangement of collocation points and choosing an exact number of expressions N in approximation series (42) in dependence on the length of segments r. It constitutes a very significant advantage as segments r may have diverse lengths when we use corner points in the modelling of boundary geometry by PIES. In order to obtain accurate results on each segment, it is necessary merely to choose N dependent on the length of segment r and the complexity of the posed boundary conditions.

The method of approximating boundary functions is very effective especially from the point of view of the analysis of the convergence of solutions. To carry it out, we should change only number N from series (42), which stands for the number of accepted expressions. From a practical point of view the process is much easier than another discretization of the domain or boundary into smaller elements.

Having found the functions on the boundary, we can obtain the solution in domain Ω on the basis of the integral identity (36).

6. Practical application of the method

In this paper the proposed method has been tested using a number of testing examples. The examples were chosen in such a way as to make it possible to define the boundary geometry by means of corner points. Another important criterion of choosing the examples is the existence of exact solutions. The above criterion limits the variety of practical boundary problems but it is necessary for testing the accuracy of the obtained solutions based on the proposed method. The effectiveness of the method compared with the traditional numerical methods such as BEM and Galerkin symmetrical BEM (SGBEM) is illustrated on the examples with numerical solutions.

6.1. Example 1

In first example, shown in Fig. 2, we consider a square domain with the Dirichlet boundary conditions. Only four corner points P_0, P_1, P_2, P_3 are required to define the boundary geometry. An important feature of the method is the fact that number of the posed points is constant and independent of the surface area of the domain. The effectiveness of the method, from point of view of boundary geometry modelling, compared with FEM and BEM, is greater with the increase of the surface area of the considered domain.

The analytical solution for this problem with a Young's modulus of unity and a Poisson's ratio of $v = 0.25$ is presented by the following functions (Aluru, 2000):

$$u_1 = x_1, \quad u_2 = -\frac{1}{4}x_2. \tag{44}$$

Displacements in some points in the domain in comparison with analytical results are presented in Table 1.

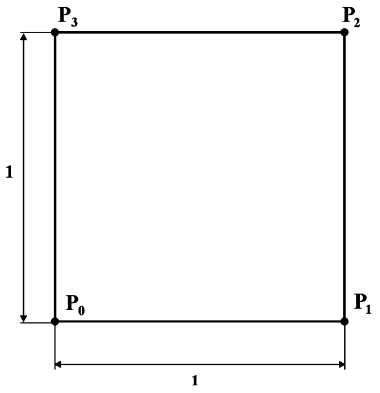

Fig. 2. Investigated domain defined by four corner points (P_0, P_1, P_2, P_3) in the PIES.

Table 1
Solutions in chosen points of the domain

Points		Exact solutions		PIES		Relative error [%]	
x_1	x_2	u_1	u_2	u_1	u_2	u_1	u_2
1	2	3	4	5	6	7	8
0.5	0.05	0.5	−0.0125	0.5	−0.012499	0.0	0.0056
0.5	0.10	0.5	−0.0250	0.5	−0.024998	0.0	0.0044
0.5	0.15	0.5	−0.0375	0.5	−0.037498	0.0	0.0032
0.5	0.20	0.5	−0.0500	0.5	−0.049998	0.0	0.0026
0.5	0.25	0.5	−0.0625	0.5	−0.062498	0.0	0.0019
0.5	0.30	0.5	−0.0750	0.5	−0.074999	0.0	0.0013
0.5	0.35	0.5	−0.0875	0.5	−0.087499	0.0	0.0009
0.5	0.40	0.5	−0.1000	0.5	−0.099999	0.0	0.0005
0.5	0.45	0.5	−0.1125	0.5	−0.112500	0.0	0.0000
0.5	0.50	0.5	−0.1250	0.5	−0.125000	0.0	0.0000
0.5	0.55	0.5	−0.1375	0.5	−0.137500	0.0	0.0000
0.5	0.60	0.5	−0.1500	0.5	−0.150001	0.0	0.0006
0.5	0.65	0.5	−0.1625	0.5	−0.162501	0.0	0.0006
0.5	0.70	0.5	−0.1750	0.5	−0.175001	0.0	0.0005
0.5	0.75	0.5	−0.1875	0.5	−0.187501	0.0	0.0005
0.5	0.80	0.5	−0.2000	0.5	−0.200001	0.0	0.0005
0.5	0.85	0.5	−0.2125	0.5	−0.212501	0.0	0.0004
0.5	0.90	0.5	−0.2250	0.5	−0.225001	0.0	0.0004
0.5	0.95	0.5	−0.2375	0.5	−0.237501	0.0	0.0056

As seen in the table the relative error that occurs in the considered cross-section is very small. In both components of the displacement the average value of relative error is almost 0%.

6.2. Example 2

In this testing example we consider a cantilever beam of $l = 10$ in length and $h = 2$ in height as shown in Fig. 3. The beam is subjected to a bending load.

Exact solutions for the beam in a plane strain are described by the following formulas (Panzeca and Salerno, 2000):

$$u_1 = -\frac{1-v^2}{Eh} q(l+x_1)x_2, \quad u_2 = \frac{1}{2Eh} q[(1-v^2)(l+x_1)^2 + v(1+v)x_2^2]. \tag{45}$$

To obtain solutions on the beam boundary, we use the PIES represented by formula (24). Only four corner points P_0, P_1, P_2, P_3 are required to define the boundary geometry in the PIES. Next, we declare in the program that the solutions on the horizontal longer edges be searched by means of the approximation series made

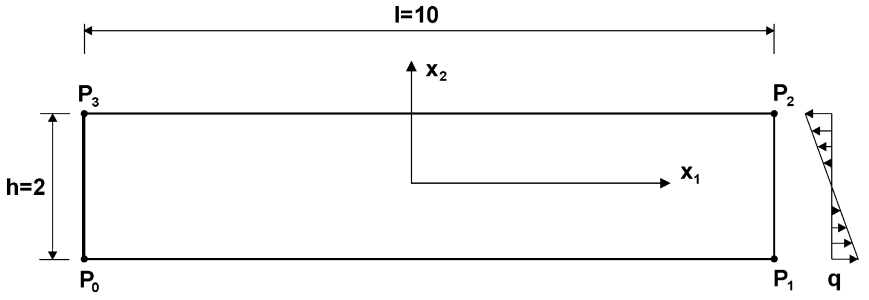

Fig. 3. Cantilever beam subjected to bending load.

Table 2
Displacements on the cantilever beam boundary

Point		Exact solution		PIES		Relative error [%]	
x_1	x_2	u_1	u_2	u_1	u_2	u_1	u_2
1	2	3	4	5	6	7	8
−4	−1	2	1.2499992	2.00000	1.25000	0.000000	6.4000E-05
−3	−1	4	4.2499973	4.00005	4.25004	0.001250	0.00100517
−2	−1	6	9.2499941	6.00009	9.25013	0.001500	0.00146940
−1	−1	8	16.249990	8.00011	16.2502	0.001375	0.00129477
0	−1	10	25.249984	10.0001	25.2504	0.001000	0.00164815
1	−1	12	36.249977	12.0002	36.2505	0.001667	0.00144331
2	−1	14	49.249968	14.0002	49.2507	0.001428	0.00148532
5	−0.8	16	100.15994	16.0001	100.161	0.000625	0.00106240
5	−0.6	12	100.08994	12.0001	100.091	0.000833	0.00106310
5	−0.4	8	100.03994	8.00006	100.041	0.000750	0.00106360
5	−0.2	4	100.00994	4.00003	100.011	0.000750	0.00106390
5	0.0	0	99.999936	−3.3E-12	100.001	–	0.00106400
5	0.2	−4	100.00994	−4.00003	100.011	0.000750	0.00106390
5	0.4	−8	100.03994	−8.00006	100.041	0.000750	0.00106360
4	1	−18	81.249948	−18.0003	81.2511	0.001667	0.00141784
3	1	−16	64.249959	−16.0002	64.2509	0.001250	0.00146477
2	1	−14	49.249968	−14.0002	49.2507	0.001428	0.00148532
1	1	−12	36.249977	−12.0002	36.2505	0.001667	0.00144331
0	1	−10	25.249984	−10.0001	25.2504	0.001000	0.00164815
−1	1	−8	16.249990	−8.00011	16.2502	0.001375	0.00129477
−2	1	−6	9.2499941	−6.00009	9.25013	0.001500	0.00146940

up of 10 terms ($N = 10$), whereas on the vertical edges of four terms. The obtained solutions for displacements u_1 and u_2 at some chosen points on the boundary as compared with exact solutions are shown in Table 2. In the calculations we assume the following material constants $E = 1440$ and Poisson ratio $v = 0.2$ and maximum value of linear load $q = 3000$.

As can be seen from the relative error shown in columns (7) and (8) the results in both tables are very accurate. An additional advantage of the proposed method is that the results are obtained by solving a small system of algebraic equations. The system of 56 algebraic equations was solved.

Having found the functions on the boundary we can obtain the solution u_1 and u_2 in domain. In order to do it, integral identity (36) is required. The obtained numerical results are compared with analytical results by calculating relative errors, as shown in Fig. 4.

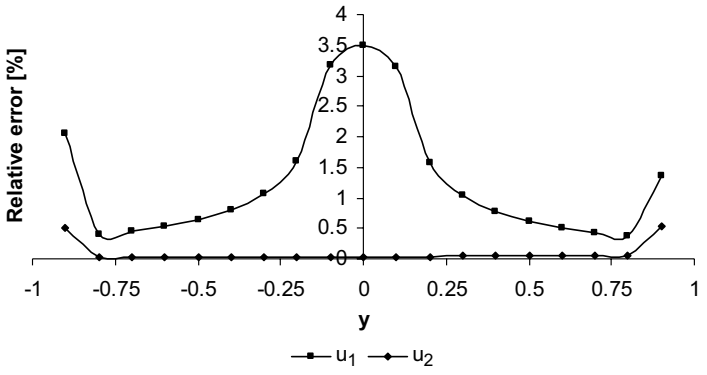

Fig. 4. Values of relative errors of obtained solutions in considered cross-section.

The greatest efficiency and originality of the proposed method lies, however, in the fact that it needs neither finite nor boundary elements to define the cantilever beam. It needs only a minimum number of input data i.e. the coordinates of four corner points. The accuracy of the solutions depends on the number N of terms adopted for the approximating series (42). To increase the accuracy of the solutions, it is only necessary to modify the value of N in the program. This way of increasing accuracy is more effective than another boundary or domain discretization for a larger number of finite (or boundary) elements.

6.3. Example 3

In this example we consider a cantilever beam of length $l = 6$ and height $h = 2$ subjected to a parabolic distribution of shear tractions along the side $x = l$ (Fig. 5). The coefficient that expresses l/h ratio amounts to 3.

Numerical results for the beam with such a load were obtained by Panzeca et al. (2001), who used symmetrical Galerkin BEM (SGBEM). Analytical solutions for displacements are presented in the following form:

$$u_1 = \frac{3(1-\nu^2)}{4Eh^3}(3l - x_1)(l + x_1)x_2, \quad u_2 = \frac{(1-\nu^2)}{4Eh^3}(5l - x_1)(l + x_1)^2. \tag{46}$$

Table 3 shows the numerical results obtained by the method proposed here at the same points as in Panzeca et al. (2001). Known analytical solution (46) enables us to compute relative errors for each result.

As can be seen in Table 3, there is a greater disproportion between average errors for both components of displacement in the case of SGBEM (column 5, 6) than in the PIES (column 7, 8). Generally the average error for both components of displacement in SGBEM method amounts to 4.94%, whilst in PIES it is equal to 3.95%.

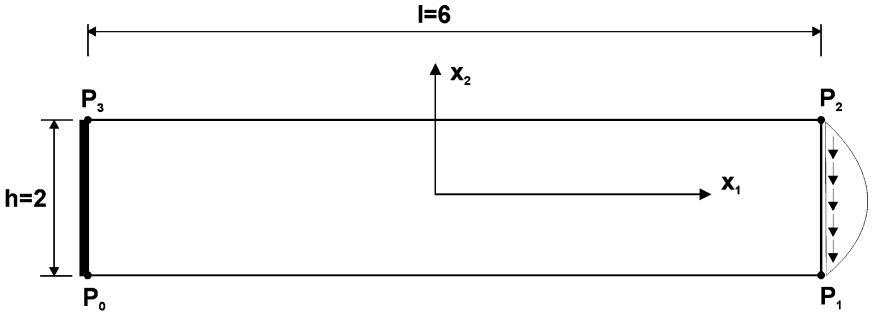

Fig. 5. A cantilever beam subjected to shearing load.

Table 3
Displacements on the cantilever beam boundary

Points		Exact solutions		SGBEM		PIES	
x_1	x_2	u_1	u_2	u_1	u_2	u_1	u_2
1	2	3	4	5	6	7	8
−3	1	0	0	–	–	–	–
0	1	18.4275	−30.7125	17.56	−33.65	17.0766	−32.182
3	1	24.57	−98.28	24.57	−103.9	−23.3801	−98.9652
3	0	0	−98.28	6.46×10^{-14}	−102.75	−1.02E−11	−98.6
3	−1	−24.57	−98.28	−24.57	−103.9	−23. 3801	−98.9652
0	−1	−18.4275	−30.7125	−17.56	−33.65	17.0766	−32.182
−3	−1	0	0	–	–	–	–
Average relative errors [%]				2.35	7.02	6.08	2.25
				4.94		3.95	

Table 4
Displacements on the cantilever beam boundary

Points		Exact solutions		PIES		Relative error [%]	
x_1	x_2	u_1	u_2	u_1	u_2	u_1	u_2
1	2	3	4	5	6	7	8
3	−0.5	−98.28	−786.24	−101.914	−766.125	3.697599	2.558379
3	−0.4	−78.624	−786.24	−80.9893	−765.698	3.008369	2.612688
3	−0.3	−58.968	−786.24	−60.4575	−765.383	2.525946	2.652752
3	−0.2	−39.312	−786.24	−40.1808	−765.165	2.210012	2.680479
3	−0.1	−19.656	−786.24	−20.0554	−765.036	2.03195	2.696886
3	0	0	−786.24	4.75E-11	−764.994	–	2.702228
3	0.1	19.656	−786.24	20.0554	−765.036	2.03195	2.696886
3	0.2	39.312	−786.24	40.1808	−765.165	2.210012	2.680479
3	0.3	58.968	−786.24	60.4575	−765.383	2.525946	2.652752
3	0.4	78.624	−786.24	80.9893	−765.698	3.008369	2.612688
3	0.5	98.28	−786.24	101.914	−766.125	3.697599	2.558379
Average relative error						2.694775	2.645873

Next the same example was solved assuming that the new height of the beam is only half of the previous height $h = 1$, and ratio $l/h = 6$. Table 4 presents displacements on the vertical edge subjected to a parabolic distribution of shear tractions (Fig. 5).

In the example the solutions are characterized by satisfactory accuracy and both components of displacement have similar average errors. Having obtained the solution on the boundary after solving the PIES, we can look for solutions in the domain. For that purpose an expression (36) should be used. Table 5 presents displacements at some chosen points in the domain.

As presented in columns 7 and 8, the values of displacements at each point of the domain are characterized by small relative errors.

6.4. Example 4

In this example, we compare the accuracy of solutions obtained using the method proposed here with exact solutions obtained by other numerical methods.

We consider a square plate 2×2 with the material constants $E = 1$ and Poisson ratio $v = 0.3$, subjected to two different loadings: a unit uniform normal load (Fig. 6a) and a bending load (Fig. 6b) acting along a single side of the plate. The analytical results are (Panzeca et al., 2001):

Table 5
Displacements in the domain

Points		Exact solutions		PIES		Relative error [%]	
x_1	x_2	u_1	u_2	u_1	u_2	u_1	u_2
1	2	3	4	5	6	7	8
0	−0.4	−58.968	−245.7	−57.7195	−237.135	2.11725	3.485958
0	−0.3	−44.226	−245.7	−43.0035	−238.301	2.764211	3.011396
0	−0.2	−29.484	−245.7	−28.608	−237.917	2.971103	3.167684
0	−0.1	−14.742	−245.7	−14.25	−237.683	3.337403	3.262922
0	0	0	−245.7	0.089438	−237.604	–	3.295075
0	0.1	14.742	−245.7	14.4285	−237.679	2.126577	3.26455
0	0.2	29.484	−245.7	28.7855	−237.909	2.369082	3.17094
0	0.3	44.226	−245.7	43.1793	−238.289	2.366707	3.01628
0	0.4	58.968	−245.7	57.8931	−237.12	1.822853	3.492063
Average relative error						2.484398	3.240763

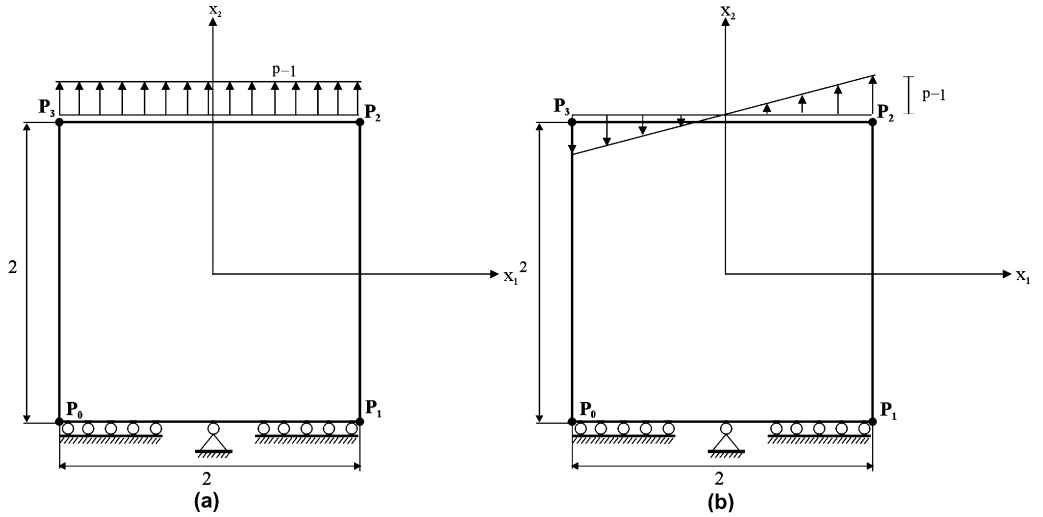

Fig. 6. A square plate subjected to (a) a uniform normal load and (b) a bending load.

$$u_1 = -0.39x_1, \quad u_2 = 0.91(x_2 + 1),$$
$$\sigma_1 = 0, \quad \sigma_2 = -1, \tag{47}$$

for the tension problem and

$$u_1 = -0.195x_1^2 - 0.455(x_2 + 1)^2, \quad u_2 = 0.91x_1(x_2 + 1),$$
$$\sigma_1 = 0, \quad \sigma_2 = x_1, \tag{48}$$

for the bending problem.

The results for individual displacements obtained on the boundary by PIES compared to exact solutions are shown in Table 6 (for uniform load) and Table 7 (for bending load). In the proposed method only four corner points are used to model the geometry of the plate. Additionally, to compare the accuracy of the method Tables 6 and 7 give the numerical results obtained by Panzeca et al. (2001) using Galerkin symmetrical BEM (SGBEM) and also the results obtained by Huang and Cruse (1994) using other numerical methods.

As can be seen all the results for each method are of high accuracy. A great advantage of the method proposed here is the fact that the domain modelling is carried out using only corner points with no need to perform boundary discretization. Another advantage of the method are continuous solutions obtained on the boundary.

The accuracy of the solutions in the domain was also tested. Due to the fact that there is some regularity of the solution obtained in all individual cross-sections of the domain, the solutions presented here refer only to cross-section $-1 < x_1 < 1$ and $x_2 = 0.5$. The results of the test are shown in Fig. 7.

As can be noticed in Fig. 7, the solutions from the PIES are very close to the analytical results. Even in the boundary vicinity of the considered domain the differences are very small. The average relative error obtained in the considered cross-section is almost equal to 0%.

6.5. Example 5

In the following example we consider a very long cantilever beam ($l = 200$) as compared to its height ($h = 10$). The way of loading and supporting the beam is presented in Fig. 8.

The investigated example was solved by means of BEM in paper (Besuner and Snow, 1978). In the paper the authors used the symmetry of the defined geometry and boundary conditions for numerical solutions. The solution for the symmetry was obtained after an application of linear boundary elements (L) and then, to increase accuracy, quadratic boundary elements (Q) were used.

Table 6
Displacements on the boundary of the plate subjected to unit uniform load

Point		Exact solution		PIES		SGBEM		Huang and Cruse	
x_1	x_2	u_1	u_2	u_1	u_2	u_1	u_2		
1	2	3	4	5	6	7	8	9	10
1	−0.75	−0.39	0.2275	−0.390003	0.22746	–	–	–	–
1	−0.50	−0.39	0.4550	−0.390005	0.45497	–	–	–	–
1	−0.25	−0.39	0.6825	−0.390006	0.68248	–	–	–	–
1	0.00	−0.39	0.9100	−0.390007	0.90998	−0.38999	0.91000	−0.39017	0.91038
1	0.25	−0.39	1.1375	−0.390008	1.13749	–	–	–	–
1	0.50	−0.39	1.3650	−0.390009	1.36500	–	–	–	–
1	0.75	−0.39	1.5925	−0.390012	1.59251	–	–	–	–
0.75	1	−0.2925	1.82	−0.292515	1.81997	–	–	–	–
0.50	1	−0.1950	1.82	−0.195009	1.81997	–	–	–	–
0.25	1	−0.0975	1.82	−0.097504	1.81997	–	–	–	–
0.00	1	0	1.82	−6.96E−14	1.81998	1.02×10^{-14}	1.82000	8×10^{-16}	1.8203
−0.25	1	0.0975	1.82	0.097504	1.81997	–	–	–	–
−0.50	1	0.1950	1.82	0.195009	1.81997	–	–	–	–
−0.75	1	0.2925	1.82	0.292515	1.81997	–	–	–	–
−1	0.75	0.39	1.5925	0.390015	1.59252	–	–	–	–
−1	0.50	0.39	1.3650	0.390009	1.36500	–	–	–	–
−1	0.25	0.39	1.1375	0.390007	1.13750	–	–	–	–
−1	0.00	0.39	0.9100	0.390007	0.90998	0.38999	0.90999	0.39017	0.91038
−1	−0.25	0.39	0.6825	0.390007	0.68248	–	–	–	–
−1	−0.50	0.39	0.4550	0.390005	0.45497	–	–	–	–
−1	−0.75	0.39	0.2275	0.390002	0.22746	–	–	–	–

Table 7
Displacements on the boundary of the plate subjected to bending load

Point		Exact solution		PIES		SGBEM		Huang and Cruse	
x_1	x_2	u_1	u_2	u_1	u_2	u_1	u_2	u_1	u_2
1	2	3	4	5	6	7	8	9	10
1	−0.75	−0.22343	0.2275	−0.22338	0.22742	–	–	–	–
1	−0.50	−0.30875	0.4550	−0.30866	0.45490	–	–	–	–
1	−0.25	−0.45093	0.6825	−0.45080	0.68238	–	–	–	–
1	0.00	−0.65000	0.9100	−0.64982	0.90986	−0.64999	0.90999	−0.64558	0.91037
1	0.25	−0.90593	1.1375	−0.90571	1.13736	–	–	–	–
1	0.50	−1.21875	1.3650	−1.21848	1.36485	–	–	–	–
1	0.75	−1.58843	1.5925	−1.58812	1.59234	–	–	–	–
0.75	1	−1.92968	1.3650	−1.92933	1.36486	–	–	–	–
0.50	1	−1.86875	0.9100	−1.86839	0.90991	–	–	–	–
0.25	1	−1.83218	0.4550	−1.83184	0.45495	–	–	–	–
0.00	1	−1.82000	0.0000	−1.81965	1.72E-16	−1.81999	-3.38×10^{-15}	−1.8166	-2.59×10^{-16}
−0.25	1	−1.83218	−0.4550	−1.83184	−0.45495	–	–	–	–
−0.50	1	−1.86875	−0.9100	−1.86839	−0.90991	–	–	–	–
−0.75	1	−1.92968	−1.3650	−1.92933	−1.36486	–	–	–	–
−1	0.75	−1.58843	−1.5925	−1.58812	−1.59234	–	–	–	–
−1	0.50	−1.21875	−1.3650	−1.21848	−1.36485	–	–	–	–
−1	0.25	−0.90593	−1.1375	−0.90571	−1.13736	–	–	–	–
−1	0.00	−0.65000	−0.9100	−0.64982	−0.90986	−0.64999	−0.90999	−0.64558	−0.91037
−1	−0.25	−0.45093	−0.6825	−0.45080	−0.68238	–	–	–	–
−1	−0.50	−0.30875	−0.4550	−0.30866	−0.45490	–	–	–	–
−1	−0.75	−0.22343	−0.2275	−0.22338	−0.22742	–	–	–	–

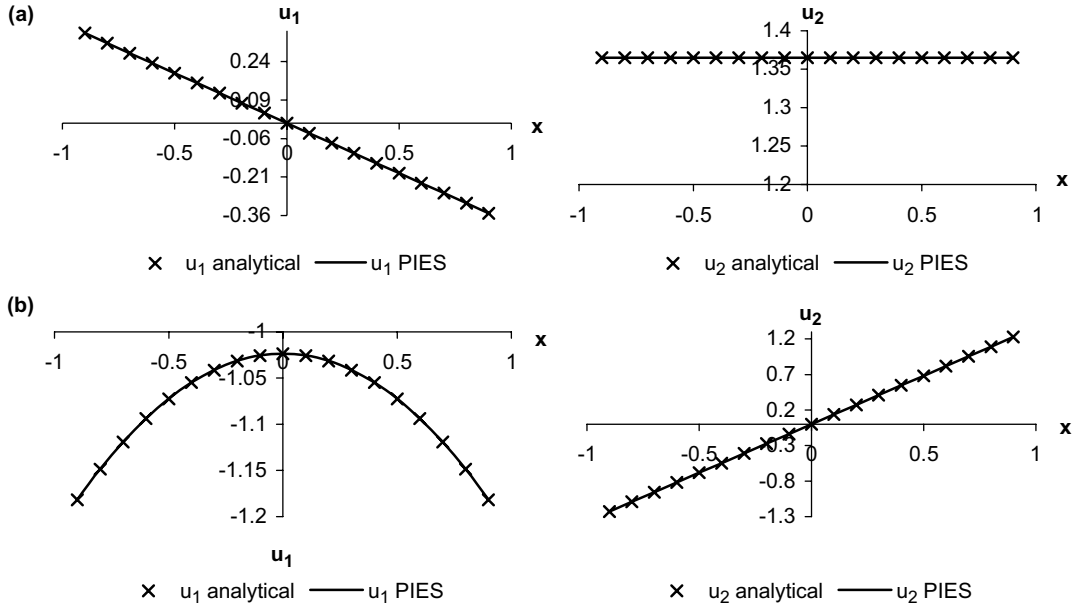

Fig. 7. Displacements in considered cross-sections for a plate subjected to (a) uniform load and (b) bending load.

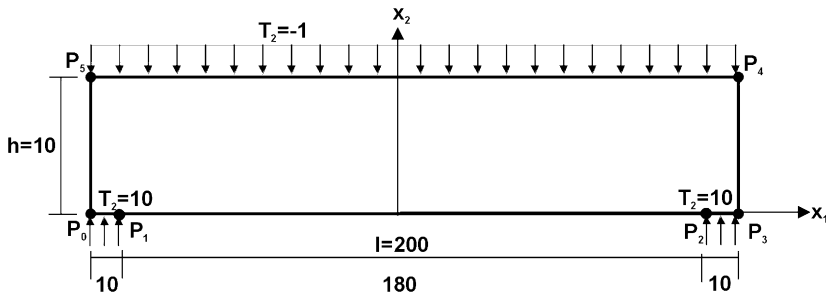

Fig. 8. Cantilever beam with uniform load.

Table 8
Normal stresses in chosen points of the domain ($x_1 = 0$)

x_2	σ_1			
	Exact	BEM (L) (error, %)	BEM (Q) (error, %)	PIES (error, %)
1	2	3	4	5
1.0	216	150 (30.555)	214 (0.925)	215.346 (0.302)
2.0	162	113 (30.246)	160 (1.234)	161.392 (0.375)
3.0	108	75 (30.555)	107 (0.925)	107.557 (0.410)
4.0	54	35 (35.185)	53 (1.851)	53.7669 (0.431)
5.0	0	−1 (–)	0 (–)	−0.002 (–)
6.0	−54	36 (33.333)	−53 (1.851)	−53.7711 (0.423)
7.0	−108	−74 (31.481)	−107 (0.925)	−107.561 (0.406)
8.0	−162	−113 (30.246)	−160 (1.234)	−161.396 (0.372)
9.0	−216	−150 (30.555)	−214 (0.925)	−215.35 (0.300)
Average error		31.519	1.234	0.378

The beam in PIES is defined merely by setting four corner points (P_0, P_3, P_4, P_5) and two additional boundary points (P_1, P_2). These points are introduced in order to account for the modification of boundary conditions. The

modeling of boundary geometry by means of corner points is very effective because the number of these points is independent of the area of the geometry considered. The presented way of posing boundary points shows that in this case we disregard the symmetry of the domain. The solutions are presented in Table 8.

The second column gives the solutions obtained by means of beam theory.

Performing an analysis of the solutions based on Table 8, it can be seen that the greatest relative error occurred in BEM when linear boundary elements were used (column 3). The value of this error is much greater than in the case of PIES (column 5). It should be also remembered that in PIES the whole domain was considered, not just the symmetry as in BEM. As can be seen in column 5, the accuracy of the results obtained by PIES is even higher than the ones obtained using quadratic boundary elements (column 4).

7. Conclusions

In the paper we have limited our solutions to boundary problems whose domains consisted of polygon with undefined boundary conditions. To obtain exact modelling of those domain only corner points are required. There is no need of introducing additional nodes between the points. The corner points constitute the minimum number of input data necessary to produce unequivocal modelling of the analyzed domain. A very important characteristic of this way of modelling in general is the fact that the number of points is independent of the length of the linear segments between those points. In other words, the number of the points for geometrically identical domains remains independent of their surface areas. This is a great advantage of modelling polygonal domains as compared with the traditional FEM and BEM in which the number of elements is strictly dependent on the surface area of the analyzed domain.

The originality of the PIES lies in the fact that its numerical solution is not directly reduced to the boundary geometry. Hence it is possible to investigate the convergence of obtained solutions without any intrusion into the modelling of boundary geometry. To do that, we only need to change the number of terms N in the series approximating unknown boundary functions. This method is definitely more effective than carrying out another boundary discretization using smaller boundary elements.

The testing examples given in the paper confirm high effectiveness of boundary modelling, high accuracy of the obtained results and simplicity of investigating the convergence of solutions. In spite of the fact that there are large numbers of boundary problems with polygonal domains, we should not limit ourselves to these problems exclusively. There are other practical boundary problems of more complex nature. It would be interesting to test the proposed method in more complex boundary geometries possibly by curves used in computer graphics. However, to do this requires even more investigations and a large number of tests.

Acknowledgement

Research work financed from the science budget for the years 2005–2008 – Polish Project Number 3T11F01528.

Appendix I

The obtaining of a modified fundamental boundary solution in an explicit form presented by formula (32) requires the computation of integrals in formula (28). After substituting (29) it to (28) four integrals were obtained:

$$I_1 = A\int_{R^2} e^{i(\omega_1\eta_1+\omega_2\eta_2)}\frac{1}{|\omega|^2}\,d\omega, \quad I_2 = B\int_{R^2}\frac{e^{i(\omega_1\eta_1+\omega_2\eta_2)}\omega_1^2}{|\omega|^4}\,d\omega,$$
$$I_3 = B\int_{R^2}\frac{e^{i(\omega_1\eta_1+\omega_2\eta_2)}\omega_1\omega_2}{|\omega|^4}\,d\omega, \quad I_4 = B\int_{R^2}\frac{e^{i(\omega_1\eta_1+\omega_2\eta_2)}\omega_2^2}{|\omega|^4}\,d\omega, \tag{I-1}$$

where A, B—some constants.

All integrals (I-1) are the same type and are computed using the same technique. Generally the technique is based on the application of the residual method for one of the integrals. Next the obtained expression is

reduced to an integral whose solution can be found in the tables for Laplace transformations. The first integral is an exception as it is simplest as far as the application of the residual method is concerned, however the second integral with a singular integrand function is obtained. To solve it the tables in Bryczkov and Prudnikov (1977) are used.

The method of calculating integral I_1: integral I_1 can be presented in the following way:

$$I_1 = A\int_{R^2} \frac{e^{i(\omega_1\eta_1+\omega_2\eta_2)}}{|\omega|^2}\,d\omega = A\int_{R^2} \frac{e^{i(\omega_1\eta_1+\omega_2\eta_2)}}{|\omega_1^2+\omega_2^2|}\,d\omega = A\int_{-\infty}^{+\infty} e^{i\omega_1\eta_1}\,d\omega_1 \int_{-\infty}^{+\infty} \frac{e^{i\omega_2\eta_2}\,d\omega_2}{|\omega_1^2+\omega_2^2|}. \tag{I-2}$$

To compute the second integral (I-2) the residual method was applied and the following expression was obtained:

$$\int_{-\infty}^{+\infty} \frac{e^{i\omega_2\eta_2}\,d\omega_2}{|\omega_1^2+\omega_2^2|} = \pi\frac{e^{-|\eta_2\|\omega_1|}}{|\omega_1|}. \tag{I-3}$$

After substituting (I-3) into (I-2) and some transformations the following singular integral was obtained:

$$I_1 = A\pi\int_{-\infty}^{+\infty} \frac{e^{i\omega_1\eta_1-|\eta_2\|\omega_1|}}{|\omega_1|}\,d\omega_1 = 2A\pi\int_0^{+\infty} \frac{\cos(\omega_1\eta_1)e^{-|\eta_2\|\omega_1|}}{|\omega_1|}\,d\omega_1. \tag{I-4}$$

Using the tables in Bryczkov and Prudnikov (1977) we can present integrals (I-4) as follows:

$$I_1 = 2A\pi\int_0^{+\infty} \frac{\cos(\omega_1\eta_1)e^{-|\eta_2\|\omega_1|}}{|\omega_1|}\,d\omega_1 = -2A\pi\left(\frac{1}{2}\ln(\eta_1^2+\eta_2^2)+F\right). \tag{I-5}$$

Remaining integrals (I-1) are calculated in a similar way, with one difference, namely that these integrals, after applying the residual method, could be reduced to integrals that have solutions in tables for Laplace transformations. The method is presented below illustrated by a more complex integral than integrals (I-1).

Appendix II

Modified singular boundary solution in an explicit form (33) is obtained after computing integral (31). Finally the following integrals should be calculated:

$$\begin{aligned}
I_5 &= -iA\int_{R^2} \frac{e^{i(\omega_1\eta_1+\omega_2\eta_2)}\omega_1}{|\omega|^2}\,d\omega, \quad I_6 = -iA\int_{R^2} \frac{e^{i(\omega_1\eta_1+\omega_2\eta_2)}\omega_2}{|\omega|^2}\,d\omega,\\
I_7 &= -iB\int_{R^2} \frac{e^{i(\omega_1\eta_1+\omega_2\eta_2)}\omega_1^3}{|\omega|^4}\,d\omega, \quad I_8 = -iB\int_{R^2} \frac{e^{i(\omega_1\eta_1+\omega_2\eta_2)}\omega_2^3}{|\omega|^4}\,d\omega,\\
I_9 &= -iB\int_{R^2} \frac{e^{i(\omega_1\eta_1+\omega_2\eta_2)}\omega_1^2\omega_2}{|\omega|^4}\,d\omega, \quad I_{10} = -iB\int_{R^2} \frac{e^{i(\omega_1\eta_1+\omega_2\eta_2)}\omega_2^2\omega_1}{|\omega|^4}\,d\omega,
\end{aligned} \tag{I-6}$$

These integrals are the same type as (I-1), but they have more complex integrand functions. The method of integration is presented for I_7

$$\begin{aligned}
I_7 &= -iB\int_{R^2} \frac{e^{i(\omega_1\eta_1+\omega_2\eta_2)}\omega_1^3}{|\omega|^4}\,d\omega = -iB\int_{R^2} \frac{e^{i(\omega_1\eta_1+\omega_2\eta_2)}\omega_1^3}{|\omega_1^2+\omega_2^2|^2}\,d\omega = -iB\int_{-\infty}^{+\infty} e^{i\omega_1\eta_1}\omega_1^3\,d\omega_1 \int_{-\infty}^{+\infty} \frac{e^{i\omega_2\eta_2}\,d\omega_2}{|\omega_1^2+\omega_2^2|^2}\\
&= -iB\int_{-\infty}^{+\infty} e^{i\omega_1\eta_1}\omega_1^3\,d\omega_1 2\pi i\left\{\frac{i|\eta_2|}{4i^2|\omega_1|^2} - \frac{2}{8i^3|\omega_1|^3}\right\}e^{-|\eta_2\|\omega_1|}\\
&= \frac{B\pi}{2}\left\{\frac{|\eta_2|}{i}\int_{-\infty}^{+\infty} \omega_1 e^{i\omega_1\eta_1^{-|\eta_2\|\omega_1|}}\,d\omega_1 + \frac{1}{i}\int_{-\infty}^{+\infty} \mathrm{sgn}(\omega_1)e^{i\omega_1\eta_1^{-|\eta_2\|\omega_1|}}\,d\omega_1\right\}\\
&= B\pi\left\{|\eta_2|\int_0^{+\infty} \omega_1\sin(\omega_1\eta_1)e^{-|\eta_2\|\omega_1|}\,d\omega_1 + \int_0^{+\infty} \sin(\omega_1\eta_1)e^{-|\eta_2\|\omega_1|}\,d\omega_1\right\},
\end{aligned}$$

where

$$\int_0^{+\infty} e^{-|\eta_2||\omega_1|} \sin(\omega_1\eta_1)\,d\omega_1 = \frac{2|\eta_2|\eta_1}{[\eta_1^2+\eta_2^2]^2}, \int_0^{+\infty} e^{-|\eta_2||\omega_1|} \sin(\omega_1\eta_1)\,d\omega_1 = \frac{\eta_1}{\eta_1^2+\eta_2^2}.$$

The remaining integrals are calculated in an analogical way.

References

Aluru, N.R., 2000. A point collocation method based on reproducing kernel approximations. International Journal of Numerical Methods in Engineering 47, 1083–1121.

Banerjee, P.K., Butterfield, R., 1981. Boundary Element Methods in Engineering Science. McGraw-Hill, London.

Besuner, Ph.M., Snow, D.W., 1978. Application of the two-dimensional integral equation method to engineering problems. In: Crusoe, T.A., Pizzo, F.J. (Eds.), Boundary-Integral Equation Method: Computational Applications in Applied Mechanics. Mir, Moskwa, pp. 129–151 (in Russian).

Brebbia, C.A., Telles, J.C.F., Wrobel, L.C., 1984. Boundary Element Techniques, Theory and Applications in Engineering. Springer, New York.

Bryczkov, J.A., Prudnikov, A.P. 1977. Integralnyje preobrazovanija obobszczonnych funkcij. Nauka, Główna Redakcja Matematyczno-Fizycznej Literatury, Moskwa (in Russian).

Camp, C.V., Gipson, G.S., 1991. Overhauser elements in boundary element analysis. Mathematical and Computer Modelling 15 (3–5), 59–69.

Durodola, J.F., Fenner, R.T., 1990. Hermitian cubic boundary elements for two-dimensional potential problems. International Journal of Numerical Methods in Engineering 30, 1051–1062.

Fletcher, C.A.J., 1984. Computational Galerkin Methods. Springer-Verlag, New York.

Gray, L.J., Soucie, C.S.A., 1993. Hermite interpolation algorithm for hypersingular boundary integrals. International Journal of Numerical Methods in Engineering 36, 2357–2367.

Huang, G., Cruse, T.A., 1994. On the non-singular traction-BIE in elasticity. International Journal of Numerical Methods in Engineering 37, 2041–2072.

Jonston, P.R., 1996. Second order overhauser elements for boundary element analysis. Mathematical and Computer Modelling 26, 61–74.

Jonston, P.R., 1997. C^2-continuous elements for boundary element analysis. International Journal of Numerical Methods in Engineering 40, 2087–2108.

Lebedev, N.N., Skalskaya, I.P., Uflayand, Y.S., 1979. Worked Problems in Applied Mathematics. Dover publications, Inc., New York.

Liggett, J.A., Salmon, J.R., 1981. Cubic spline boundary elements. International Journal of Numerical Methods in Engineering 17, 543–556.

Panzeca, T., Salerno, M., 2000. Macro-elements in the mixed boundary value problems. Computational Mechanics 26, 437–446.

Panzeca, T., Fujita Yashima, H., Salerno, M., 2001. Direct stiffness matrices of BEs in the Galerkin BEM formulation. European Journal of Mechanics/A Solids 20, 277–298.

Sen, D.A., 1995. Cubic-spline boundary integral method for two-dimensional free-surface flow problems. International Journal of Numerical Methods in Engineering 38, 1809–1830.

Singh, K.M., Kalra, M.S., 1995. Application of cubic Hermitian algorithms to boundary element analysis of heat conduction. International Journal of Numerical Methods in Engineering 38, 2639–2651.

Timoshenko, S.P., Goodier, J.N., 1970. Theory of Elasticity. McGraw-Hill, Tokyo.

Zieniuk, E., 2001. Potential problems with polygonal boundaries by a BEM with parametric linear functions. Engineering Analysis with Boundary Elements 25, 185–190.

Zieniuk, E., 2002. A new integral identity for potential polygonal domain problems described by parametric linear functions. Engineering Analysis with Boundary Elements 26 (10), 897–904.

Zieniuk, E., 2003. Bézier curves in the modification of boundary integral equations (BIE) for potential boundary-values problems. International Journal of Solids and Structures 40 (9), 2301–2320.

Zieniuk, E., Bołtuć, A., 2004. An algorithm for numerical solving of the two-dimensional Helmholtz equation using a parametric integral equations systems (PIES). Structures–Waves–Human Health XIII (1), 157–164.

Zieniuk, E., Bołtuć, A. 2005. De Boor control points for effective identification of smooth boundaries in inverse boundary problems solved by PIES. In: Proceedings of Computer Methods in Mechanics, Częstochowa, on CD, p. 6.

Zieniuk, E., Bołtuć, A., Szerszeń, K., 2004. Numerical solving of Parametric Integral Equations System (PIES) using Chebyshev's collocation method for Laplace's equation with Dirichlet boundary conditions on polygonal domains. Archiwum Informatyki Teoretycznej i Stosowanej 16 (1), 17–31 (in Polish).

Zienkiewicz, O., 1977. The Finite Element Methods. McGraw-Hill, London.